Making the Case for Predictive Thermal Management of Fuel Cell Systems for Electrified Vehicles

Making the Case for Predictive Thermal Management of Fuel Cell Systems for Electrified Vehicles

Pier Giuseppe Anselma[1,2], Sara Luciani[1,2], Andrea Tonoli[1]
[1]Department of Mechanical and Aerospace Engineering (DIMEAS), Politecnico di Torino, Torino, Italy
[2]Center for Automotive Research and Sustainable Mobility (CARS), Politecnico di Torino, Torino, Italy

E-mail: pier.anselma@polito.it

***Abstract*- This paper investigates the potential of predictive thermal management as hydrogen saving enabler for Fuel Cell Electric Vehicles (FCEVs). First, a numerical approach to model the fuel cell system of the FCEV from energy and thermal perspectives is described. A rule-based reactive approach is then considered as baseline controller for the instantaneous radiator fan state and the coolant rate of the FCEV. Subsequently, an optimal predictive thermal management strategy is implemented based on the global optimal principle of dynamic programming (DP). The fuel cell system is simulated while the FCEV performs a 93 kilometer long drive cycle considering different ambient temperatures that respectively represent summer, mid-season, and winter cases. Both baseline reactive thermal management and optimal predictive thermal management approaches are considered in this case. Results highlight how predictive thermal management can enable up to more than 8% hydrogen saving compared with the baseline reactive controller. The viability and usefulness of predictive thermal management for FCEVs is demonstrated in this way.**

I. INTRODUCTION

The deployment of hybrid electric and pure electric vehicle technologies has been proposed as a viable approach for decarbonizing conventional cars (i.e. that are powered by internal combustion engines alone) [1]. However, the drawbacks of these technologies (e.g. reliance on fossil fuels, limited range, slow recharging rate) have paved the way for the use of other energy sources in electrified vehicles. In this context, proton exchange membrane (PEM) fuel cells are a promising option thanks to high energy density, zero emissions, and extended operating temperature range [2].

The stack temperature plays a key role in PEM fuel cell systems [3]. On the one hand, high temperatures boost catalyst activity on the gas diffusion layer, speeding up the process. However, as the temperature further rises, the fuel cell membrane starts dehydrating, causing the ohmic drop to increase considerably. On the other hand, the reaction rate excessively slows down if the stack temperature is too low, resulting in a lack of electrical power [4]. Thus, a proper thermal management system is required to optimize the performance of the fuel cell system, i.e. to save hydrogen by reducing the overall power consumption of the auxiliaries while keeping the fuel cell system temperature within a safe operating range [5].

Fuel cell system themal management approaches from the literature are usually of reactive type. For example, Binrui et al. proposed a fuzzy incremental proportional-integral-derivative approach to control the temperature of a PEM fuel cell [6]. Han et al. investigated different control algorithms to adapt the PEM fuel cell stack temperature to the reference value in transient phenomena [5]. In 2019, Lohse-Busch et al. presented experimental data for the 2016 Toyota Mirai fuel cell electric vehicle (FCEV) by assessing the performance of the fuel cell system reactive thermal control logic at different ambient temperatures [7]. On the other hand, predictive thermal management approaches are emerging that exploit the prediction of future operating conditions (e.g. by means of traffic or road information) to reduce hydrogen consumption of FCEVs [8]. For example, Hahn et al. recently proposed a model predictive control (MPC) thermal management strategy for a FCEV based on a 0.4 second prediction horizon [9]. Nevertheless, the developed predictive controller was not benchmarked with the respective global optimal solution. Indeed, a systematic approach to assess the potential of predictive thermal management for FCEVs in terms of optimal hydrogen saving still requires extensive development in the mentioned literature. This consideration inspired the present work, which aims at defining how much hydrogen can be saved by implementing an optimal predictive thermal management approach to control the instantaneous radiator fan state and the coolant rate of the fuel cell system of a FCEV. The paper is organized as follows: the fuel cell thermal model and the baseline reactive control strategy are presented. Then, a global optimal predictive thermal management approach based on dynamic programming (DP) is introduced. The potential of predictive thermal management as hydrogen saving enabler is then evaluated by simulating the FCEV in a 93-kilometer long drive cycle at different ambient temperatures and by benchmarking with the baseline reactive thermal controller. Finally, the conclusions are given.

II. FUEL CELL THERMAL MODEL AND BASELINE CONTROL STRATEGIES

This section describes the numerical model of the fuel cell and its cooling system, along with the baseline rule-based reactive thermal control strategy. Here, the numerical approach

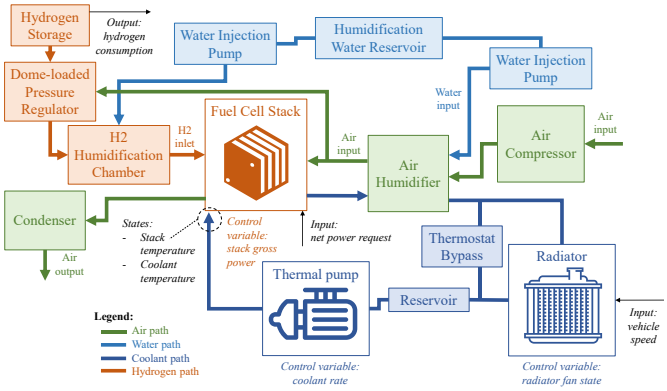

Fig. 1 Schematic diagram of the fuel cell system including fuel cell stack and auxiliary system.

for modeling the fuel cell system is transient and semi-empirical. It has been developed by Virginia Tech in collaboration with National Renewable Energy Laboratory (NREL) and implemented in the Advisor™ 2003 simulation tool embedded in Matlab® software [10]. Fig. 1 illustrates a schematic diagram of the retained fuel cell system highlighting the interaction between the components of the system. In the following up of this section, the model inputs will be described first. Then, the electrochemistry model of the fuel cell stack will be detailed. The following part will illustrate the thermal model of the fuel cell stack along with the modelling of the electrical power consumption of the auxiliary system components. Finally, the net electrical power provided by the fuel cell system will be evaluated.

A. Model inputs

Looking at Fig. 1, at each time instant of the driving mission, the numerical model receives as input current values of the vehicle speed and the net electrical power that the fuel cell system is required to provide. The value of vehicle speed allows evaluating the heat exchange between the radiator and the coming air. The considered FCEV is a passenger car, and it is propelled by an electric motor coupled to the wheels through a direct drive. Both the fuel cell system and a battery pack can provide electrical power to the electric motor. The electrical power split between the fuel cell system and the high-voltage battery pack is thus controlled at each time instant by the vehicle supervisory control algorithm. In this paper, the net fuel cell system power request is evaluated according to a rule-based thermostatic vehicle supervisory control logic implemented in Advisor™ 2003 [11].

B. Electrochemistry model

The electrochemistry model allows fulfilling two main purposes as regards assessing the operating conditions of the fuel cell system:

1) Determine the system electrical operating conditions in terms of voltage and current density along with the H2 mass flow rate;
2) Evaluate the heat generated by the system, which is in turn fed to the thermal model.

In this framework, an iterative solver needs implementation to make sure that the net electrical power generated by the fuel cell system balances the corresponding vehicle power request. An initial guess is required for the stack current density I_{stack}. Then, the cell voltage V_{cell} can be determined using the polarization equation developed by Nelson and reported in (1):

$$V_{cell}(I_{stack}, T_{stack}, p_{O2}) = OCV_{cell} - V_{tafel}(I_{stack}) - V_{ohmic}(I_{stack}, T_{stack}) - V_{concentration}(I_{stack}, p_{O2}) + V_{temperature}(I_{stack}, T_{stack}) \quad (1)$$

where OCV_{cell} and V_{tafel} are the cell open-circuit voltage and a term related with activation voltage loss as a function of the stack current density. V_{ohmic} stands for a voltage drop term related to resistance or ohmic losses in the cell as a function of the stack current density and temperature T_{stack} in kelvin as provided by the thermal model. $V_{concentration}$ accounts for the concentration of mass transportation losses in the cell as a function of the stack current density and the oxygen partial pressure at the cathode inlet p_{O2}. Finally, $V_{temperature}$ considers the effects of the stack temperature on the cell voltage. The gross fuel cell system power $P_{stack-gross}$ in watts can then be obtained using (2):

$$P_{stack-gross} = I_{stack} \cdot OCV_{cell} \cdot A_{cell} \cdot n_{cell} \quad (2)$$

where A_{cell} and n_{cell} are the area of a single cell in centimetres square and the number of cells contained in the stack, respectively. Once the value of $P_{stack-gross}$ is known, the H2 mass flow rate $\dot{m}_{H2}$ in kilograms per second can be evaluated using (3) [12].

$$\dot{m}_{H2} = \frac{P_{stack-gross} \cdot 1.05e^{-8}}{V_{cell}} \quad (3)$$

Finally, the instantaneous heat generated by the stack (Q_{stack}) can be obtained using (4):

$$Q_{stack} = \dot{m}_{H2} \cdot LHV_{H2} - P_{stack-gross} \quad (4)$$

where LHV_{H2} stands for the hydrogen lower heating value which is assumed being 1.1968e8 J/Kg here.

C. Thermal model of the stack and auxiliay power consumption

Looking at Fig. 1, modelling the thermal behaviour of the fuel cell stack and the electrical power consumption of the auxiliary systems involves six main components represented by the air compressor, the coolant pump, the radiator fan, and the condenser fan along with the fuel cell stack and the humidifier. In general, the thermal model receives as instantaneous input the heat generated by the fuel cell system, the vehicle longitudinal speed, and the current values of temperatures. Each component is then modelled according to energy and mass balances to enable evaluating the corresponding outlet temperatures and electrical power consumptions.

Concerning the air compressor, the air mass flow rate and the air pressure are needed to evaluate its contribution in the parasitic power use. The air pressure at the compressor outlet (i.e. the stack inlet) is obtained by interpolating in a one-dimensional experimental lookup table which is provided as a function of the stack current. On the other hand, the air flow

rate ($\dot{m}_{air}$) in kilograms per second can be evaluated according to the instantaneous values for stack gross power and cell voltage using the following equation [12]:

$$\dot{m}_{air} = \frac{3.57e{-}7 \cdot SR_{air} \cdot P_{stack-gross}}{V_{cell}} \quad (5)$$

where SR_{air} is the air stoichiometric ratio. Empirical lookup tables are consequently used to evaluate the adiabatic efficiency ($\eta_{adiabatic}$) and the temperature rise of the compressor as a function of the air flow rate ($\dot{m}_{air}$) and the related ratio between inlet and ambient air pressures (p_{ratio}). Then, the air compressor electrical power consumption ($P_{compressor}$) is evaluated using (6):

$$P_{compressor}(\dot{m}_{air}, T_{amb}, p_{ratio}) = \frac{\dot{m}_{air} \cdot c_{p,air}(T_{amb}) \cdot T_{amb} \cdot p_{ratio}^{\frac{k-1}{k}-1}}{\eta_{elec} \cdot \eta_{adiabatic}(\dot{m}_{air}, p_{ratio})} \quad (6)$$

where $c_{p,air}$ and k stand for the air specific heat as a function of the ambient temperature T_{amb}, and the specific heat ratio for the air, respectively. η_{elec} is the compressor motor drive electrical efficiency which is assumed having a constant value here.

When it comes to the radiator, two one-dimensional lookup tables are considered that map the heat transfer coefficient between coolant and external air (h_{rad}) as a function of the vehicle speed ($speed_{veh}$) for the radiator fan being activated or de-activated, respectively [13]. The radiator fan state is considered in the binary variable $state_{fan}$. Then, the temperature of the coolant at the radiator outlet ($T_{coolant,out}$) can be calculated as follows:

$$T_{coolant,out} = T_{coolant,in} - 0.5 \cdot \frac{A_{rad} \cdot h_{rad}(speed_{veh}, state_{fan}) \cdot (T_{coolant,in} - T_{amb})}{\dot{m}_{coolant} \cdot c_{p,coolant}} \quad (7)$$

where $T_{coolant,in}$ is the coolant temperature at the radiator inlet and equals the value of $T_{coolant,out}$ in the previous time instant. $\dot{m}_{coolant}$ is the coolant mass flow rate through the coolant pump, while $c_{p,coolant}$ is the specific heat of the coolant. A_{rad} stands for the radiator frontal area, while the 0.5 constant in (7) accounts for the numerical model being initially calibrated for a 0.5 m^2 radiator. When activated, the radiator fan is assumed here constantly consuming a 300 watts electrical power ($P_{radiator-fan}$).

Coolant is circulated through the fuel cell system thanks to the coolant pump, which moves energy through the stack, humidifier, and radiator. The instantaneous heat removed by the coolant ($Q_{coolant}$) can be calculated using (8):

$$Q_{coolant} = \dot{m}_{coolant} \cdot c_{p,coolant} \cdot (T_{stack} - T_{coolant,out}) \quad (8)$$

From an electrical point of view, the parasitic power consumed by the coolant pump ($P_{coolant-pump}$) can be obtained by interpolating in a one-dimensional lookup table as a function of $\dot{m}_{coolant}$.

The stack temperature in the next time instant ($T_{stack,next}$) can be determined according to the thermal balance reported in (9):

$$\begin{aligned} T_{stack,next} &= T_{stack} \\ &+ (Q_{stack} - Q_{coolant} - Q_{ambient} - Q_{air} \\ &- Q_{water-vapor} + Q_{condenser}) \cdot \frac{\Delta t}{L_{lumped}} \end{aligned}$$

with

$$\begin{aligned} Q_{ambient} &= h_{stack} \cdot (T_{stack} - T_{amb}) \\ Q_{air} &= \dot{m}_{air} \cdot c_{p,air} \cdot (T_{air,in} - T_{stack}) \\ Q_{water-vapor} &= \dot{m}_{wv-in} \cdot c_{p,wv}(T_{wv,in}) - \dot{m}_{wv-out} \\ &\cdot c_{p,wv}(T_{stack}) \\ Q_{condenser} &= \dot{m}_{H20,condensed} \cdot h_{fg} \end{aligned} \quad (9)$$

where Δt and L_{lumped} are the simulation time step in seconds and the lumped stack thermal capacitance in joules per kelvin, respectively. $Q_{ambient}$ is the overall heat transferred from the stack to the ambient by means of natural convection. In this term, h_{stack} is the overall heat transfer coefficient associated with natural convection. Q_{air} is the heat contribution brought by the air provided by the compressor at temperature $T_{air,in}$. $Q_{water-vapor}$ accounts for the enthalpy variation of water and vapor between inlet and outlet of the stack. In this term, $\dot{m}_{wv-in}$ and $\dot{m}_{wv-out}$ are the mass flow rates of water and vapor entering and exiting the stack, respectively. $c_{p,wv}$ is the corresponding specific heat for water and vapor which is evaluated for temperatures $T_{wv,in}$ and T_{stack}, respectively. $Q_{condenser}$ is the heat exchanged between stack and condenser, which can be evaluated considering the mass flow rate of the condensed water ($\dot{m}_{H20,condensed}$) and the heat of vaporization of water (h_{fg}).

D. Net system power

The last step of the implemented fuel cell system modelling approach involves determining the net electrical power provided by the system. This is achieved by performing an electrical power balance subtracting the overall auxiliary losses from the system gross power as reported in (10):

$$P_{stack-net} = P_{stack-gross} - P_{compressor} - P_{coolant-pump} - P_{radiator-fan} - P_{condenser-fan} \quad (10)$$

where $P_{condenser-fan}$ is the power consumption of the condenser fan, which is assumed here being 300 watts when the fuel cell system is in operation.

Finally, the value of $P_{stack-net}$ is compared with the net power request evaluated in sub-section 2.1. In case of a mismatch, a solver is implemented to iteratively adjust the value of stack current density until comparable values are obtained between the power requested and the power provided. The interested reader can consult [10] to obtain more information regarding the implemented approach for modelling the fuel cell system.

E. Baseline reactive thermal control strategy

The baseline reactive thermal control strategy is required to set at each time instant the values for the radiator fan state, the coolant mass flow rate provided by the pump, and the gross power of the fuel cell stack.

The baseline reactive control strategy activates the radiator fan as soon as the value of stack inlet temperature exceeds the

operating temperature set point, which corresponds to 80° C. Then, the radiator fan is kept operating as long as the value of stack inlet temperature is greater than 80°.

As far as the thermal pump is concerned, one of its operating requirements involves limiting the temperature rise across the fuel cell for practical reasons. The baseline reactive thermal control strategy assumes that all the internal energy generated is transferred to the coolant. Then, the coolant mass flow rate in kilograms per second can be determined as follows:

$$\dot{m}_{coolant} = \frac{Q_{stack}}{c_{p,coolant} \cdot \Delta T_{allowed}} \quad (11)$$

where $\Delta T_{allowed}$ is the maximum amount of temperature rise that the fuel cell can tolerate, which is calibrated as 8° C for the vehicle considered in Advisor™ 2003.

The final control variable is the fuel cell stack gross power, which is iteratively adjusted in the baseline reactive control strategy until the net power provided by the fuel cell system as evaluated in (10) fulfills the corresponding vehicle power request.

III. Predictive Thermal Management Approach

This section describes the implemented approach for assessing the potential of predictive thermal management as a hydrogen saving enabler for FCEVs. Dynamic programming (DP) is considered as a widely adopted optimal control approach for dynamic systems [14][15]. DP can find the global optimal control solution of the considered problem by operating an exhaustive sweep of all discretized control and state values at each simulation time instant. Global optimality is ensured thanks to the a priori knowledge of the system operating conditions (i.e. vehicle speed and net stack power request) over the entire driving mission [16]. Here, the DP algorithm is set to minimize the overall hydrogen consumption for the entire driving mission. Three control variables are considered as reported in Fig. 1, namely the stack gross power, the radiator fan state, and the coolant rate. State variables whose values are tracked over the entire control problem relate here to the stack temperature and to the coolant temperature. The full control variable set U and the state variable set X for the fuel cell system thermal control problem under investigation are illustrated in (12):

$$U = \begin{Bmatrix} \frac{P_{stack-gross}}{P_{stack-request}} \\ state_{fan} \\ \dot{m}_{coolant} \end{Bmatrix} \; ; \; X = \begin{Bmatrix} T_{stack} \\ T_{coolant} \end{Bmatrix} \quad (12)$$

Several optimization constraints are considered in the implementation of the DP algorithm. The net electrical power delivered by the fuel cell system (equal to the difference between controlled gross power and the power consumed by the auxiliary systems including compressor, radiator fan, thermal pump, and condenser fan) is constrained to be equal or higher than the net power request. The temperature of the stack is set not to exceed the maximum allowed limit (95° C here). Finally, all the fuel cell system components are constrained to operate within respective allowed ranges. The open-source 'DynaProg' DP function implemented in Matlab® is used in this work for solving the illustrated optimal control problem for thermal management of fuel cell systems [17].

IV. Simulation Results at Different Ambient Temperatures

This section compares simulation results obtained at different ambient temperatures. In particular, the predictive thermal management approach represented by DP is benchmarked with the baseline reactive thermal control strategy inherited from Advisor™ 2003. The potential in terms of hydrogen saving achievable by implementing predictive thermal management can be evaluated in this way. Table I shows FCEV parameters inherited from Advisor™ and retained in this study. Both reactive and predictive thermal management approaches have been simulated that correspond to the rule-based thermal control strategy inherited by Advisor™ and to the global optimal control obtained using DP. Four repetitions of the Worldwide Harmonized Light Vehicle Test Cycle (WLTC) are considered (i.e. a 93 km journey), and three ambient temperatures are simulated, namely 30° C (summer case), 10° C (mid-season case), and -5° C (winter case). Fig. 2 shows obtained time series in the simulation of the summer case, while Table II reports statistics for the simulations of all the three season cases. 6.0% to 8.1% hydrogen saving is demonstrated to be achievable by the FCEV thanks to predictive thermal management in correspondence with summer and winter cases, respectively.

Fig. 3 illustrates the efficiency map and the operating points of the fuel cell stack for both reactive and predictive fuel cell thermal management approaches. The average position of the stack operating points for the reactive thermal control approach noticeably depends on the value of ambient temperature and are shifted downwards towards lower efficient areas as the ambient temperature decreases. On the other hand, the predictive control approach could preserve the stack operation in highly efficient operating areas at each assessed value of ambient temperature.

Fig. 4 highlights the energy saving contribution terms for the predictive thermal management approach compared to the baseline reactive approach, which can be obtained by comparing the corresponding values in Table II. Overall, the major contributors to the overall hydrogen saving entailed by

TABLE 1: FCEV PARAMETERS

Component	Parameter	Value
Vehicle	Mass	1500 kg
	Frontal area	2.0 m^2
	Drag coefficient	0.335
	Tyre radius	0.282 m
Electric motor	Maximum power	75 kW
Transmission	Ratio	6.67
Battery pack	Nominal voltage	292 V
	Capacity	7.4 Ah
Fuel cell system	Maximum power	55 kW
	Cell area	678 cm^2
	Number of cells	210
	Max cell voltage	0.94 V

TABLE II: STATISTICS FOR THE FUEL CELL SYSTEM SIMULATED BEING CONTROLLED BY REACTIVE AND PREDICTIVE THERMAL CONTROL STRATEGIES IN FOUR REPETITIONS OF WLTC

		$T_{amb} = 30° C$ (summer)		$T_{amb} = 10° C$ (mid)		$T_{amb} = -5° C$ (winter)	
		Reactive (rule-based)	**Predictive (DP)**	**Reactive (rule-based)**	**Predictive (DP)**	**Reactive (rule-based)**	**Predictive (DP)**
Energy loss [kJ]	Compressor energy	6180	5839	5878	5302	5609	4972
	Thermal pump energy	2454	614	2461	250	2465	228
	Radiator fan energy	1689	300	1657	67	1256	45
	Condenser fan energy	1313	1313	1313	1313	1313	1313
	Stack chemical loss	39298	36322	40860	35585	41665	35439
Energy generation [kJ]	Stack power request	58978	58978	58978	58978	58978	58978
	Gross stack power generation	70613	67044	70279	65910	69602	65536
Statistics	Stack average efficiency [%]	64.2	64.9	63.2	64.9	62.6	64.9
	Fuel cell system average efficiency [%]	53.7	57.1	53.1	58.1	53.0	58.4
	H2 consumption [kg]	0.92	0.86	0.93	0.85	0.93	0.84
	H2 saving [%]	-	6.0	-	7.7	-	8.1

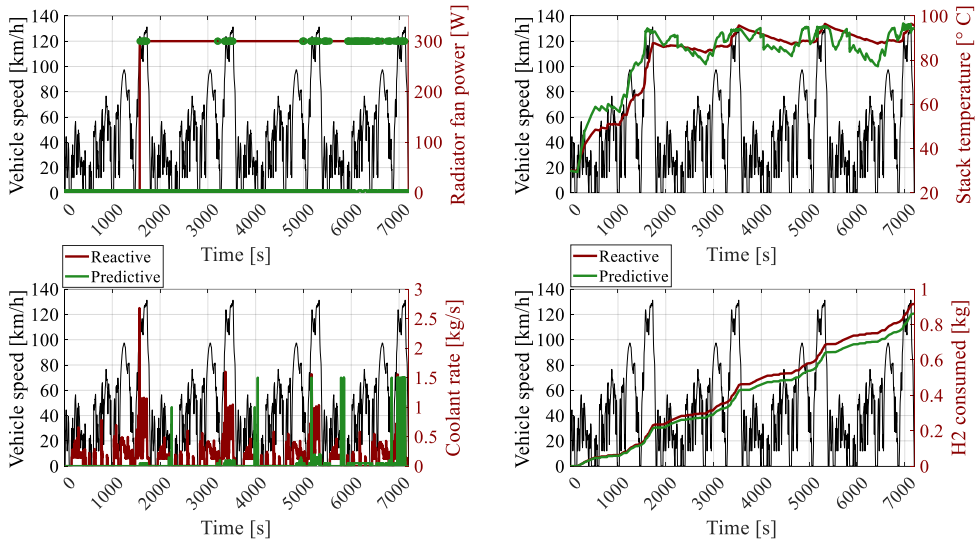

Fig. 2 Time series of vehicle speed radiator fan power, stack temperature, coolant rate and H2 consumption for both reactive and predictive fuel cell thermal management approaches in four repetitions of WLTC at ambient temperature equal to 30° C (summer case).

the predictive DP thermal control strategy in order of magnitude correspond to 1) the improved fuel cell stack efficiency (i.e. the stack chemical loss reduction), 2) the auxiliary power loss reduction of the thermal pump, 3) the auxiliary power loss reduction of the radiator fan, and 4) the auxiliary power loss reduction of the compressor. In this framework, the stack chemical loss matches the heat generated by the stack and it can be evaluated using (4). Reduced utilization of the radiator fan and the coolant pump are predicted by DP being hydrogen saving enablers, as shown in Fig. 2 for example. In particular, the optimal control behavior predicted by DP is observed remarkably reducing the overall radiator fan ON time compared with the baseline reactive control strategy. Moreover, DP activates the radiator fan in Fig. 2 only at high values of vehicle speed as in highway driving, which considerably improves the efficiency of the heat removal process within the radiator. As it can be seen Table I and in Fig. 4, the predictive thermal management approach also reduces the auxiliary energy consumed by the air compressor. The air compressor is the most energy demanding auxiliary component of the fuel cell system. Its air mass flow rate is not considered here as a variable controlled by DP, but rather its value over time is set according to the baseline reactive control approach. However, reducing the gross power required by the fuel cell system is demonstrated to bring significant benefits concerning the power consumption of the air compressor as it was shown in (5) and in (6). Such virtuous loop can be listed among the key benefits brought by the proposed optimal thermal control approach in terms of hydrogen saving.

V. CONCLUSIONS

This study assesses the potential of predictive thermal management as a hydrogen saving enabler for FCEVs through numerical simulations. Various ambient temperatures are considered representing summer, mid-season, and winter

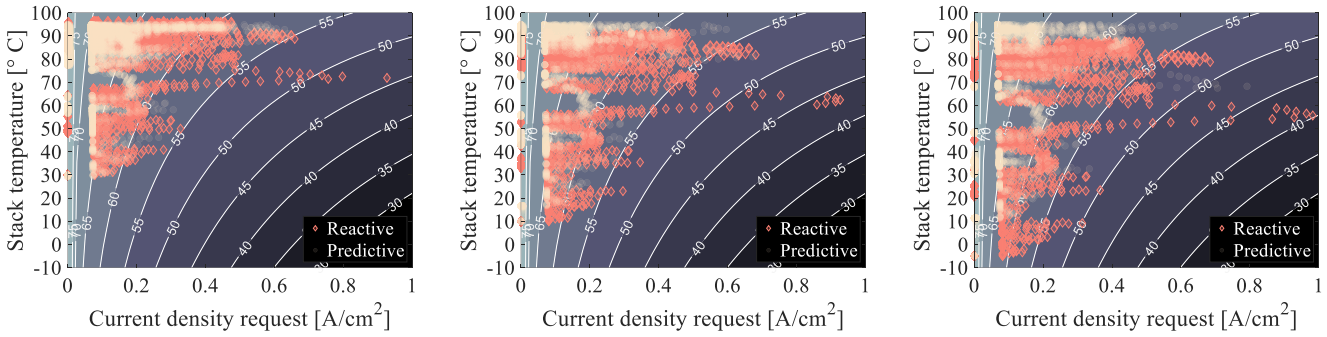

(c) T_{amb} = 30° C (b) T_{amb} = 10° C (a) T_{amb} = -5° C

Fig. 3 Efficiency map and operating points of the fuel cell stack for both reactive and predictive fuel cell thermal management approaches in four repetitions of WLTC at ambient temperatures equal to -5° C (winter case), 10° C (mid-season case) and 30° C (summer case).

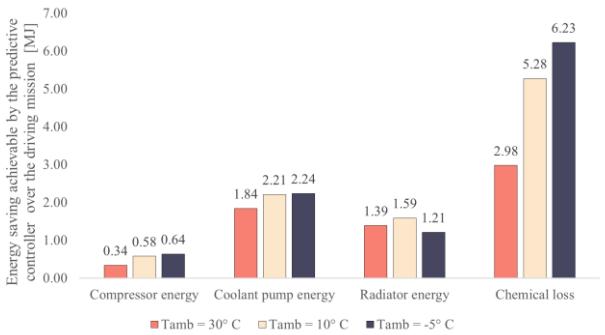

Fig. 4 Predicted energy saving contributions for the predictive thermal management approach compared to the baseline reactive approach in four repetitions of WLTC at ambient temperatures equal to -5° C (winter case), 10° C (mid-season case) and 30° C (summer case).

cases. DP is implemented as global optimal predictive thermal management approach, while a reactive rule-based thermal controller is retained as benchmark. Obtained results demonstrate the potential of predictive thermal management by showing that through its implementation a FCEV can save 6% to 8% hydrogen in a 93-kilometer journey in correspondence with summer and winter cases, respectively. It should be noted that in this work the potential of a predictive thermal management approach for fuel cell systems in FCEVs in terms of hydrogen savings has been assessed in an off-line approach assuming a priori complete knowledge of the entire future driving conditions. Related future work could involve developing real-time capable predictive thermal management approaches for FCEVs. In this case, the profile of the vehicle velocity over time may not match with the initially predicted counterpart. The presented DP off-line algorithm could provide the optimal benchmark and an off-line optimized training dataset for the predictive thermal management approaches to be developed.

REFERENCES

[1] M. Kandidayeni, A. Macias, L. Boulon, S. Kelouwani, “Investigating the impact of ageing and thermal management of a fuel cell system on energy management strategies,” *Applied Energy*, vol. 274, no. 115293, 2020.

[2] C. Acar, I. Dincer, “The potential role of hydrogen as a sustainable transportation fuel to combat global warming,” *International Journal of Hydrogen Energy*, vol. 45, no. 5, pp. 3396-3406, 2020.

[3] S. Cheng, L. Xu, K. Wu, C. Fang, J. Hu, J. Li, M. Ouyang, “Optimal warm-up control strategy of the PEMFC system on a city bus aimed at improving efficiency,” *International Journal of Hydrogen Energy*, vol. 42, no. 16, pp. 11632-11643, 2017.

[4] B. Zhang, F. Lin, C. Zhang, R. Liao, Y.X. Wang, “Design and implementation of model predictive control for an open-cathode fuel cell thermal management system,” *Renewable Energy*, vol. 154, pp. 1014-1024, 2020.

[5] J. Han, S. Yu, S. Yi, “Advanced thermal management of automotive fuel cells using a model reference adaptive control algorithm”, *International Journal of Hydrogen Energy*, vol. 42, no. 7, pp. 4328-4341, 2017.

[6] W. Binrui, J. Yinglian, X. Hong, W. Ling, "Temperature control of PEM fuel cell stack application on robot using fuzzy incremental PID," *2009 Chinese Control and Decision Conference*, pp. 3293-3297, 2009.

[7] H. Lohse-Busch, K. Stutenberg, M. Duoba, X. Liu, A. Elgowainy, M. Wang et al., “Automotive fuel cell stack and system efficiency and fuel consumption based on vehicle testing on a chassis dynamometer at minus 18° C to positive 35° C temperatures,” *International Journal of Hydrogen Energy*, vol. 45, no. 1, pp. 861-872, 2020.

[8] W. Na, T. Park, T. Kim and S. Kwak, "Light Fuel-Cell Hybrid Electric Vehicles Based on Predictive Controllers," in *IEEE Transactions on Vehicular Technology*, vol. 60, no. 1, pp. 89-97, Jan. 2011.

[9] S. Hahn, J. Braun, H. Kemmer, H.C. Reuss, “Adaptive operation strategy of a polymer electrolyte membrane fuel cell air system based on model predictive control”, *International Journal of Hydrogen Energy*, *46*(33), 17306-17321, 2021.

[10] S. D. Gurski, “Cold-start effects on performance and efficiency for vehicle fuel cell systems”, *M. Sc. thesis, Virginia Tech*, 2002.

[11] T. Markel, A. Brooker, T. Hendricks, V. Johnson, K. Kelly, B. Kramer, B. et al., “ADVISOR: a systems analysis tool for advanced vehicle modeling”, *Journal of power sources*, vol. 110, no. 2, pp. 255-266, 2002.

[12] J. Larminie, A. Dicks, M.S. McDonald, “Fuel cell systems explained”, *Chichester, UK: J. Wiley*, 2003.

[13] D. G. Kröger, “Radiator Characterization and Optimization,” *SAE Transactions*, vol. 93, pp. 984–90, 1984.

[14] J. Lempert, B. Vadala, K. Arshad-Aliy, J. Roeleveld and A. Emadi, "Practical Considerations for the Implementation of Dynamic Programming for HEV Powertrains," *2018 IEEE Transportation Electrification Conference and Expo (ITEC)*, 2018, pp. 755-760.

[15] D. Zhou, F. Gao, A. Ravey, A. Al-Durra and M. G. Simões, "Online energy management strategy of fuel cell hybrid electric vehicles based on time series prediction," *2017 IEEE Transportation Electrification Conference and Expo (ITEC)*, 2017, pp. 113-118.

[16] P. G. Anselma, P. Kollmeyer, G. Belingardi and A. Emadi, "Multi-Objective Hybrid Electric Vehicle Control for Maximizing Fuel Economy and Battery Lifetime," *2020 IEEE Transportation Electrification Conference & Expo (ITEC)*, 2020, pp. 1-6.

[17] F. Miretti, D. Misul, E. Spessa, “DynaProg: Deterministic Dynamic Programming solver for finite horizon multi-stage decision problems,” *SoftwareX*, vol. 14, no. 100690, 2021.